THE JOURNAL OF BIOLOGICAL CHEMISTRY
Vol. 280, No. 17, Issue of April 29, pp. 17135–17141, 2005
Printed in U.S.A.

An Activation Switch in the Rhodopsin Family of G Protein-coupled Receptors

THE THYROTROPIN RECEPTOR*

Received for publication, December 30, 2004, and in revised form, February 15, 2005
Published, JBC Papers in Press, February 18, 2005, DOI 10.1074/jbc.M414678200

Eneko Urizar‡§¶, Sylvie Claeysen‡, Xavier Deupí‖, Cedric Govaerts‡, Sabine Costagliola‡, Gilbert Vassart‡, and Leonardo Pardo‖

From the ‡Institut de Recherche Interdisciplinaire en Biologie Humaine et Nucléaire, Université Libre de Bruxelles, Campus Erasme, 808 route de Lennik, B-1070 Bruxelles, Belgium, the ‖Laboratori de Medicina Computacional, Unitat de Bioestadística and Institut de Neurociències, Universitat Autònoma de Barcelona, 08193 Bellaterra, Spain, and the §Departamento de Neurofarmacología, Facultad de Farmacia, Universidad del País Vasco, 1006 Vitoria-Gasteiz, Spain

We aimed at understanding molecular events involved in the activation of a member of the G protein-coupled receptor family, the thyrotropin receptor. We have focused on the transmembrane region and in particular on a network of polar interactions between highly conserved residues. Using molecular dynamics simulations and site-directed mutagenesis techniques we have identified residue Asn-7.49, of the NP*xx*Y motif of TM 7, as a molecular switch in the mechanism of thyrotropin receptor (TSHr) activation. Asn-7.49 appears to adopt two different conformations in the inactive and active states. These two states are characterized by specific interactions between this Asn and polar residues in the transmembrane domain. The inactive *gauche*+ conformation is maintained by interactions with residues Thr-6.43 and Asp-6.44. Mutation of these residues into Ala increases the constitutive activity of the receptor by factors of ~14 and ~10 relative to wild type TSHr, respectively. Upon receptor activation Asn-7.49 adopts the *trans* conformation to interact with Asp-2.50 and a putatively charged residue that remains to be identified. In addition, the conserved Leu-2.46 of the (N/S)L*xxx*D motif also plays a significant role in restraining the receptor in the inactive state because the L2.46A mutation increases constitutive activity by a factor of ~13 relative to wild type TSHr. As residues Leu-2.46, Asp-2.50, and Asn-7.49 are strongly conserved, this molecular mechanism of TSHr activation can be extended to other members of the rhodopsin-like family of G protein-coupled receptors.

Genome sequencing projects have identified the G protein-coupled receptor (GPCR)[1] family as one of the largest class of proteins with more than 800 human sequences. These sequences have been classified into five main families, glutamate, rhodopsin, adhesion, frizzled/taste2, and secretin (1). GPCRs are involved in passing chemical signals across the cell membrane. The incoming signal may arrive in the form of neurotransmitters, peptides, divalent cations, proteases, hormones, and sensory stimuli such as photons and gustatory or odorant molecules (2, 3). Atomic level details of a three-dimensional structure of a GPCR are only known for the inactive form of rhodopsin, the light photoreceptor protein of rod cells (4, 5). Rhodopsin is formed by an extracellular N terminus, seven α-helices, which cross the cellular membrane (TM 1–TM 7) connected by hydrophilic loops, and a cytoplasmic C terminus containing an α-helix (HX 8) parallel to the cell membrane. The overall structure of the helical bundle seems common in the rhodopsin-like GPCR family because of the large number of conserved sequence patterns in these 7 TM segments (6): GN in TM 1, (N/S)L*xxx*D in TM 2, (D/E)RY in TM 3, CW*x*P in TM 6, and NP*xx*Y$(x)_{5,6}$F in TM 7 and HX 8, among others.

Activation of GPCRs is commonly discussed in terms of the extended ternary complex model, which proposes an equilibrium between inactive and active states (7). Recent advances in the β_2-adrenergic receptor have shown that agonist binding, leading to the active form of the receptor, is a multistep process (8–10). Agonist binding or constitutively active mutations disrupt a series of constraining intramolecular interactions that keep the receptor in the inactive conformation. Recently identified constraints within the transmembrane domain are i) the conformational transition of Trp of the CW*x*P motif in TM 6 (11, 12), ii) the interaction of Asn of the NP*xx*Y motif in TM 7 with either residues located in TM 6 (13) or the backbone of TM 6 through a water molecule (14), iii) the ionic lock between Arg of the highly conserved (D/E)RY motif in TM 3 and a partly conserved Asp/Glu residue in the cytoplasmic end of TM 6 (15), and iv) the aromatic-aromatic interaction between Tyr of the NP*xx*Y motif in TM 7 and an aromatic residue located in HX 8 (16, 17). Release of these constraints induce rigid body motions of several if not all transmembrane helices (18, 19).

The thyrotropin receptor (TSHr), together with the luteinizing hormone/chorionic gonadotropin and follicle-stimulating hormone receptors, is a member of the glycoprotein hormone receptor family of GPCRs. These receptors are characterized by a large N-terminal ectodomain, responsible for high affinity

* This work was supported by the Belgian State, Prime Minister's office, Service for Sciences, Technology and Culture; the Interuniversity Attraction Poles of the Belgian Federal Office for Scientific, Technical and Cultural Affairs; grants from the FRSM, FNRS, ARBD, and BRAHMS Diagnostics; the European Community Sixth Framework Programme (LSHB-CT-2003-503337); and CICYT (SAF2002-01509). The costs of publication of this article were defrayed in part by the payment of page charges. This article must therefore be hereby marked "*advertisement*" in accordance with 18 U.S.C. Section 1734 solely to indicate this fact.

¶ Predoctoral fellow from the Government of the Basque Country.

** To whom correspondence should be addressed: Unitat de Bioestadística, Facultat de Medicina, Edifici M, Campus Universitari, Universitat Autònoma de Barcelona, 08193 Bellaterra, Spain. Tel.: 3493-581-2797; Fax: 3493-581-2344; E-mail: Leonardo.Pardo@uab.es.

[1] The abbreviations used are: GPCR, G protein-coupled receptor; TSH, thyroid-stimulating hormone; TSHr, thyrotropin receptor; hTSHr, human TSHr; TM, transmembrane helix; WT, wild type; FACS, fluorescence-activating cell sorting; MD, molecular dynamics; bTSH, bovine TSH; SCA, specific constitutive activity.

binding of the hormone and by a rhodopsin-like helical bundle, responsible for signal transduction (20, 21). An interesting peculiarity of the TSHr is the wide spectrum of mutations capable of increasing its constitutive activity (22), offering a valuable tool to study molecular mechanisms of GPCR activation. We have shown that in the glycoprotein hormone receptor family an Asp residue in TM 6, maintains the highly conserved Asn (in the NP*xx*Y motif in TM 7) in the inactive state through a complex hydrogen bond network (13). Similar constraining interactions have been reported for the luteinizing hormone/chorionic gonadotropin (23, 24). Moreover, this Asn residue is crucial in the activation mechanism by both the natural agonist (13) and activating mutations, including those affecting the (E/D)RY motif that release the ionic lock between TM 3 and 6 (25). Interestingly, mutation of this Asn to Ala in the C5a receptor abrogates receptor signaling (26). Thus, Asn of the NP*xx*Y motif seems to be a key residue in the stabilization of both the inactive and active states of other receptors as well. We aim in this work to study the interactions of the Asn side chain in the inactive and active state of the TSHr by a combination of molecular modeling, functional assays, and site-directed mutagenesis.

EXPERIMENTAL PROCEDURES

Molecular Modeling and Molecular Dynamics Simulations

A model of the transmembrane domain of the TSHr plus helix 8 that expands parallel to the membrane was constructed by homology modeling using the crystal structure of bovine rhodopsin (PDB code 1L9H) as a template (14). The molecular models for the mutant receptors containing the single D2.50N (standardized nomenclature[2] (27)) or double D2.50N/N7.49D substitutions were built from the derived model of WT TSHr, by changing the atoms implicated in the amino acid substitutions by interactive computer graphics. These structures were placed in a rectangular box (~60 × 72 × 70 Å in size) containing a lipid bilayer (60 molecules of palmitoyloleoylphosphatidylcholine and ~7650 molecules of water in addition to the receptor structure), resulting in a final density of ~1.0 g cm^{-3}. The receptor-lipid bilayer systems were subjected to 500 iterations of energy minimization and then heated to 300 K in 15 ps. This was followed by an equilibration period (15–250 ps) and a production run (250–500 ps) at constant pressure with anisotropic scaling, using the particle mesh Ewald method to evaluate electrostatic interaction. During the processes of minimization, heating, and equilibration a positional restraint of 10 kcal $mole^{-1}Å^{-2}$ was applied to the C_α atoms of the receptor structure. This simulation protocol seems adequate to adapt the rhodopsin template to the structural requirements of the wild type and mutants receptor side chains, with the aim of understanding the local helix-helix interactions that keep the receptor in the inactive state. Structures were collected for analysis every 10 ps during the production run (25 structures/simulation). The molecular dynamics (MD) simulations were run with the Sander module of AMBER 8 (28), the ff99 force field (29), SHAKE bond constraints in all bonds, a 2 fs integration time step, and constant temperature of 300 K coupled to a heat bath. The molecular electrostatic potentials were calculated with GRASP (30).

Reagents

Plasmid pBluescript SK^+ was from Stratagene, plasmid pSVL was from Amersham Biosciences, restriction enzymes were from Invitrogen and New England Biolabs (Beverly, MA), and Pfu Turbo polymerase from Stratagene. Monoclonal antibody (mAb) BA8, obtained by genetic immunization (31), was directed against a conformational epitope on the TSHr ectodomain. Bovine TSH (bTSH) was from Sigma.

Construction of TSHr Mutants

Mutations were introduced in the hTSHr by site-directed mutagenesis as described previously (32). The primers are available upon request. Amplified fragments of SK^+ hTSHr containing the appropriate mutations were subcloned in pSVL hTSHr cDNA (between XhoI and XbaI restriction sites). All constructs were amplified in DH5αF′-electrocompetent cells, and recombinant DNA from selected clones was purified and sequenced for confirmation of PCR-generated fragments.

Transfection Experiments

COS-7 cells were used for all transient expression experiments, which were performed according to two different protocols (20). Briefly, 300,000 or 2 million cells were seeded in 3.5- or 10-cm Petri dishes, respectively, at day 1 and transfected based on the DEAE-dextran transfection method (32) at day 2. For the 3.5 dishes protocol, 2 days later cells were used for flow immunofluorometry and cAMP determinations; whereas for the 10-cm dishes at day 3, cells were detached by trypsinization, centrifuged, resuspended in 16 ml of culture medium and seeded in 24-well plates (1 ml/well). At day 5, cells were used for flow immunofluorometry and cAMP determinations. Duplicate dishes were used for each assay. Cells transfected with pSVL alone were always run as negative controls.

Cell Surface Expression

Expression of wt and diverse hTSHr mutants was quantified by flow immunofluorometry with the mAb BA8 exactly as described preciously (31). The fluorescence of 10,000 cells/tube was assayed by FACScan FLOW cytofluorometer (BD Biosciences). Cells transfected with pSVL alone and pSVL hTSHr were always run as negative and positive controls, respectively.

Determination of cAMP Production

For cAMP determinations, culture medium was removed 48 h after transfection and replaced by Krebs-Ringer-HEPES buffer for 30 min. Thereafter, cells were incubated for 60 min in fresh Krebs-Ringer-HEPES buffer supplemented with 25 μM phosphodiesterase inhibitor Rolipram (Laboratoire Logeais, Paris, France) in the absence or presence of various concentrations of bTSH (Sigma). The medium was discarded, replaced with 0.1 M HCl, and the extracts were dried under vacuum, resuspended in water, and diluted appropriately for cAMP measurements. Duplicate samples were assayed in all experiments; results are expressed in pmol/ml. Because of the linear relationship existing between basal cAMP accumulation and receptor cell surface expression (32), basal cAMP was normalized to cell surface expression for each of the constructs. To this end, specific cAMP accumulation (equal to cAMP of receptor-transfected cells − cAMP of the pSVL-transfected cells) is divided by the specific FACS value (equal to fluorescence of receptor-transfected cells − fluorescence of pSVL-transfected cells). Specific basal activity was defined as = (cAMP(receptor) − cAMP(pSVL))/(FACS(receptor) − FACS(pSVL)). The values were then normalized to the basal activity of the WT TSHr, arbitrarily set to 1. Concentration-effect curves were fitted with Prism v3.03 (GraphPad Software, Inc., San Diego, CA).

RESULTS

Molecular Modeling and Molecular Dynamics Simulations

Fig. 1*a* shows a detailed view of the Asp-2.50/Asn-7.49/Asp-6.44 environment of the molecular model of the TSHr in the inactive conformation obtained by unrestrained MD simulations (see "Experimental Procedures"). Importantly, the Wat_1 set of water molecules found in the most recent structure of rhodopsin (1L9H) are included in the model (14). These structural waters mediate a number of interhelical interactions through the highly conserved Asp-2.50 and Asn-7.49 amino acids. The lack of coordination of the polar Asp-2.50 in both rhodopsin and the TSHr leads us to suggest that this set of water molecules is also present in the TSHr and is putatively involved in maintaining the inactive form of the receptor. Wat_{1a} links TM 2, TM 3, and TM 7, acting as a hydrogen bond donor in the interaction between the side chain of Asp-2.50 and the backbone carbonyl of Ala-3.35 and as a hydrogen bond acceptor in the interaction with the side chain of Asn-7.45. Wat_{1b} is located between TM 2 and TM 7, linking the backbone carbonyl of Asn-7.45, the backbone N–H amide of Asn-7.49, the side chain of Asp-2.50, and the side chain of Asn-7.49. As shown in Fig. 1*a*, a network of hydrogen bond interactions restrains the side chain of Asn-7.49 in the χ_1 = *gauche*+ rotamer con-

[2] Each residue is numbered according to the helix (1 through 7) in which it is located and to the position relative to the most conserved residue in that helix, arbitrarily assigned to 50. This allows easy comparison among residues in the transmembrane segments of different receptors.

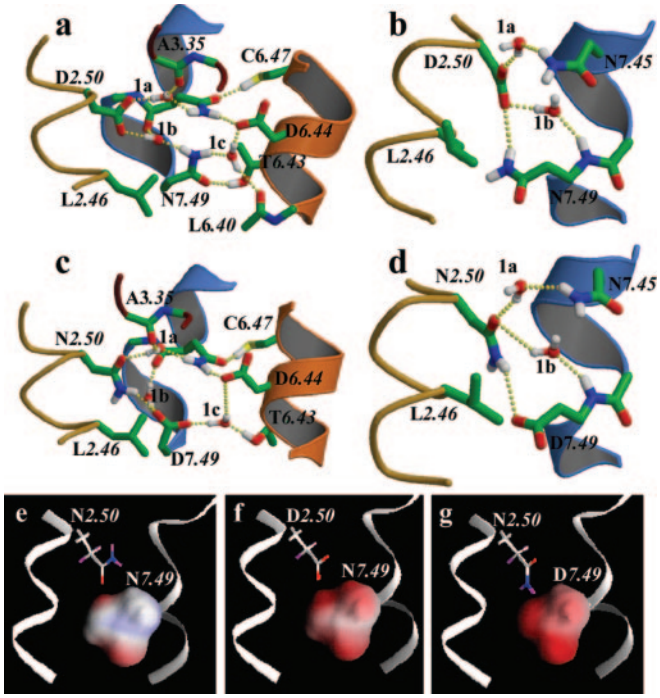

FIG. 1. **Computational models of TSH and mutant receptors.** *a–d*, a detailed view of the proposed hydrogen bond network, at the 2.50/7.49/6.44 environment, in the inactive (*a* and *c*) and active (*b* and *d*) conformations of WT TSHr (*a* and *b*) and the D2.50N/N7.49D double mutant (*c* and *d*). *e–g*, molecular electrostatic potential, with the color scale going from −5 (*red*) to +5 (*blue*), caused by the D2.50N (*e*), WT TSH (*f*), and D2.50N/N7.49D (*g*) receptor structures at the accessible surface of Asn-7.49 (*e* and *f*) or Asp-7.49 (*g*). *a–d* were created using MolScript v2.1.1 (45) and Raster3D v2.5 (46), and *e–g* were created with GRASP (30).

formation, pointing toward TM 6. In particular, both Thr-6.43 and Asp-6.44 interact with Asn-7.49 through a water molecule (Wat_{1c}). Wat_{1c} is also bridging the side chain of Asn-7.49 and the backbone carbonyl of Leu-6.40. It is important to note that Wat_{1c} is very mobile during the simulation and can also achieve, in other snapshots, interactions with other residues like Thr-6.43 or Ser-3.39. These proposed networks of interactions partly diverge from the previously described model (13) because of the presence of these functional water molecules. Finally, Asn-7.45 is interacting with Asp-6.44, Cys-6.47, and Wat_{1a}, whereas Tyr-7.42 is hydrogen bonding, via the OH group, one of the O_δ atoms of Asp-6.44 and the $O_\gamma H$ group of Ser-3.36 (not depicted for clarity). A detailed description of the role of these side chains in maintaining the inactive conformation of the homologous follicle-stimulating hormone receptor has recently been published (33).

We have previously suggested that upon receptor activation the side chain of Asn-7.49 undergoes a conformational transition from *gauche+* to *trans* (13). Fig. 1*b* shows the computer model of the TSHr where the side chain conformation of Asn-7.49 has been initially modified from its inactive *gauche+* conformation to a *trans* conformation. The recently obtained structure of metarhodopsin I has revealed that early stages of activation does not involve large rigid body movements of helices but local side chain relocations (12). Thus, this modeling exercise only aims at exploring the possible interactions of Asn-7.49 in the active state of the receptor, which could correspond to early stages of the activation process when side chain relocations have not yet been translated into major structural changes. Regardless of these limitations, it seems clear that the conformational transition of Asn-7.49 allows for a direct interaction with Asp-2.50. As a consequence the polar O_δ atom of Asn-7.49 reorients toward the intracellular side and becomes accessible. During the simulations the positively charged side chain of Arg-6.36, highly conserved within the glycoprotein hormone receptor family, hydrogen bonds the O_δ atom of Asn-7.49 (not shown). Fig. 1, *a–d*, also shows the position of the highly conserved side chain of Leu-2.46.

Experimental Results

The role of the residues theoretically predicted to interact with Asn-7.49 in its "inactive" or "active" rotamer conformation was experimentally tested by site-directed mutagenesis and functional assays (Table I, Figs. 2 and 3). The following mutants were engineered.

Thr-6.43 and Asp-6.44 Mutants—The molecular model depicted in Fig. 1*a* predicts that both Thr-6.43 and Asp-6.44 are involved in the interaction with Asn-7.49. Thus, we engineered the D6.44A, D6.44N, T6.43A, and the double T6.43A/D6.44N mutant receptors (Figs. 2 and 3). These mutants are expressed at the 26–96% range (Table I and Figs. 2*A* and 3*A*). D6.44N functions as WT TSHr in terms of constitutive activity, whereas D6.44A increases basal activity by a factor of ~14 (Table I) as was previously shown (13). Notably, T6.43A also increases basal activity by a factor of ~10 relative to WT receptor that is comparable in magnitude to the D6.44A mutant receptor (Table I). Strikingly, with a specific constitutive activity (or SCA) of ~3 (see Table I) the double T6.43A/D6.44N mutant is less constitutive than T6.43A (SCA of ~10) but higher than the WT-like D6.44N mutant (SCA of 1.1). This suggests that Thr-6.43 has a more significant role in constraining the side chain conformation of Asn-7.49 in the presence of Asp-6.44 than Asn-6.44. All the mutants are able to respond to bTSH.

Asp-2.50 and Asn-7.49 Mutants—The process of TSHr activation appears to require the release of Asn-7.49, from the interactions with the residues in TM 6, toward Asp-2.50 (13). Thus, single D2.50A, D2.50N, and N7.49D, and double D2.50N/N7.49D mutant receptors were engineered (Table I and Figs. 2 and 3) to explore the hypothesis of a direct Asp-2.50**Asn-7.49 interaction in the active state of the TSHr. These mutants are expressed at the 24–115% range (Table I and Fig. 2*A*). D2.50A and D2.50N show a loss in basal activity (Table I and Fig. 2*C*). Furthermore, the typical concentration-response curve illustrated in Fig. 3*C* for the D2.50N construct shows higher EC_{50} and lower E_{max} values than WT receptor. Thus, Asp-2.50 seems crucial to stabilize the active state of the receptor. On the other side N7.49D shows a significant increase in constitutive activity, reaching more than 11 times that of wild type TSHr (Table I and Fig. 2*C*) as was previously shown (13). Notably, addition of the D2.50N mutation on the N7.49D background, making the D2.50N/N7.49D double mutant, reverses completely the phenotype to levels of constitutive activity even below wild type-like behavior (Table I and Fig. 2*C*). Moreover, these mutants efficiently respond to bTSH (Fig. 2*B*).

Adding D6.44A to the mutant receptors already containing Asp at the 7.49 position (N7.49D *versus* N7.49D/D6.44A, D2.50N/N7.49D *versus* D2.50N/N7.49D/D6.44A) increases constitutive activity (SCA of ~11 *versus* ~16 and ~0 *versus* ~5; Table I and Fig. 2*C*). This suggests an additional role for Asp-6.44 than solely maintaining Asn-7.49 in an inactive state. The charged Asp-6.44 could also modulate the conformation of other polar side chains with possible involvement in the activation mechanism. Putative candidates are Ser-3.39, Asn-7.45, or/and Tyr-7.42.

The Arg-6.36 Mutant—Arg-6.36 was replaced by Ala to explore the possibility of a direct interaction between the Asp-2.50**Asn-7.49 pair and Arg-6.36 in the active state of the

TABLE I
Functional properties of WT TSH and mutant receptors

Level of cell surface expression (FACS), basal cAMP accumulation previous and after normalized to surface expression (SCA), maximal concentrations of bTSH-induced cAMP accumulation (E_{max}), and EC_{50} values obtained from functional dose-response curves. Values represent the mean ± S.E. of at least two independent determinations. ND, not determined; −, single measurement.

	FACS		Basal cAMP accumulation				E_{max}		EC_{50}	
	% Expression of WT		Raw values		SCA		10 mIU/ml or plateau		mIU/ml	
	Mean	S.E.	Mean	S.E.	Mean	S.E.	Mean	S.E.	Mean	S.E.
TSHr WT	100		27.90	3.24	1.00		196.81	24.45	0.19	0.10
L2.46A	12	1.33	15.99	1.48	13.06	0.86	82.97	10.24	0.12	0.0012
L2.46I	35	5.73	8.22	0.78	0.78	0.01	115.51	25.99	0.22	−
L2.46W	18	1.97	3.27	1.74	0.10	0.06	9.55	1.30	6.91	−
D2.50N	115	6.96	5.65	0.97	0.18	0.09	73.53	15.38	0.85	0.12
D2.50A	25	0.94	7.60	1.13	0.28	0.16	38.84	14.06	ND	ND
R6.36A	91	−	9.45	−	0.11	−	150.23	−	0.21	−
T6.43A	40	3.96	116.86	17.29	9.71	1.15	285.48	78.64	0.51	0.21
D6.44A	26	−	125.84	−	13.58	−	246.70	−	ND	ND
D6.44N	96	−	44.33	−	1.10	−	328.74	−	ND	ND
N7.49D	24	−	97.37	−	11.32	−	333.59	−	ND	ND
D2.50N/D6.44N	119	15.15	8.40	2.17	0.11	0.03	69.02	9.33	ND	ND
D2.50N/D6.44A	74	9.44	58.28	1.63	2.26	0.03	97.98	22.68	ND	ND
D2.50A/D6.44A	15	5.16	18.77	1.85	5.39	1.49	38.11	4.28	ND	ND
D2.50N/N7.49D	49	7.47	5.37	1.36	0.11	0.03	112.76	50.46	ND	ND
D2.50N/D6.44A/N7.49D	28	3.69	39.75	6.26	4.62	0.42	72.00	8.10	ND	ND
D6.44A/N7.49D	20	4.48	78.55	16.32	15.90	3.05	179.03	32.87	ND	ND
T6.43A/D6.44N	69	−	78.53	−	2.84	−	282.55	−	ND	ND

receptor as suggested during MD simulations. The R6.36A mutant exhibits reduced constitutive activity relative to wild type TSHr (Fig. 2*C*), but the receptor can be activated by the extracellular ligand (Fig. 2*B*). This data disregards the possibility of Arg-6.36 as the counterpart to the Asp-2.50**Asn-7.49 pair in the active state of the receptor.

Leu-2.46 Mutants—We also performed the L2.46A, L2.46I, and L2.46W mutations to investigate the role of this highly conserved Leu residue, which belongs to a conserved hydrophobic layer (34), and it is located in the proximity of Asn-7.49 in the TSHr molecular model. The cell surface expression of the L2.46A mutant is only 12% of WT receptor (Table I and Fig. 3*A*). L2.46A shows a significant increase in basal activity when normalized to surface expression (Fig. 3*B*). The concentration-response curve illustrated in Fig. 3*D* shows that L2.46A is activated efficiently by TSH with similar EC_{50} to WT receptor (Table I). Introduction of a β-branched Ile residue at this 2.46 position only shows a decrease in receptor expression at the cell surface (Table I). Basal activity and ligand-induced cAMP accumulation seem to be unaffected (Fig. 3). In contrast, L2.46W decreases basal activity, and the mutant receptor is almost unable to be activated by the hormone (Fig. 3).

DISCUSSION

Previous work (13, 25) showed the central role of Asn-7.49 in the activation of the TSHr, acting as an on/off switch by adopting two different conformations in the inactive and active states. In the present work we aimed at identifying the partners of Asn-7.49 regulating this conformational transition.

The TD6.44 Motif Restrains the Side Chain of Asn-7.49 Pointing toward TM 6 in the Inactive State of the TSHr—We have identified Thr-6.43 and Asp-6.44 as the main partners of Asn-7.49 in the inactive state of the receptor. The $O_{\gamma 1}H$ moiety of Thr-6.43 acts as hydrogen bond donor in the interaction with the $O_{\delta 1}$ atom of Asn-7.49, whereas the $O_{\delta 1}$ atom of Asp-6.44 and the $N_{\delta 2}H$ group of Asn-7.49 are linked (Fig. 1*a*). Accordingly, both D6.44A and T6.43A single mutants show a significant increase in constitutive activity relative to WT TSHr, by factors in the order of ~14 and ~10 (Table I and Fig. 2), respectively.

As the TD6.44 motif is specific to the glycoprotein hormone receptor family, the question arises of whether the inactivation of Asn-7.49 through interactions with partners in TM 6, can be extrapolated to the other members of the GPCR family. It has recently been shown that an internal water molecule in the crystal structure of rhodopsin (14) bridges the side chain of Asn-7.49 (Asn-302 in bovine rhodopsin) and the backbone carbonyl of Gly-6.40 (Gly-257), keeping the Asn side chain toward TM 6. This suggests a conserved mechanism where Asn-7.49 of the NP*xx*Y motif is restrained toward TM 6 in the inactive state of all rhodopsin-like GPCRs by intramolecular interactions that diverge among GPCR subfamilies.

*The Asp-2.50**Asn-7.49 Interaction in the Active State of the TSHr*—The modeling and experimental data presented above, together with previously reported results (13), suggest that the release of the Asn-7.49 side chain, from interactions with the Thr-6.43/Asp-6.44 residues, is a necessary step in TSHr activation. Disruption of these interactions has a large energetic cost that must be compensated by the formation of new stabilizing interactions. We propose Asp-2.50 as the most likely partner of Asn-7.49 in the active state of the TSHr (Fig. 1*b*). In this mode of interaction the polar O_{δ} atom of Asn-7.49 is free and points toward the intracellular side (see below). This carboxylate oxygen has been suggested as necessary in TSHr activation (35).

Some members of the GPCR family receptors exchange the NP*xx*Y motif by DP*xx*Y in TM 7 (6). Several works have suggested a Asp-2.50/Asn-7.49 direct interaction in the active state of GPCRs (36, 37). These two residues are found interchanged in the gonadotropin-releasing hormone receptor and engineering such a swap leads to functional receptors in a number of cases (36, 37). Notably, this D2.50N/N7.49D swapping in the TSHr leads to a mutant receptor with lower constitutive activity than WT TSHr (Fig. 2). This suggests that, despite the presence of a negative charge at both 6.44 and 7.49 positions, there is a hydrogen bond network constraining Asp-7.49 toward TM 6. Fig. 1*c* shows the molecular model of the D2.50N/N7.49D double mutant in the inactive conformation (see "Experimental Procedures"). The side chain of Asp-7.49 is interacting with Asn-2.50 and Thr-6.43 (through Wat_{1c}), whereas Asp-6.44 is coordinated by Ser-3.39, Tyr-7.42, and Asn-7.45 (not all depicted in Fig. 1*d* for clarity). This finding reinforces the hypothesis of the presence of Wat_{1c} in the Asn-7.49 environment. We suggest that activation of the D2.50N/

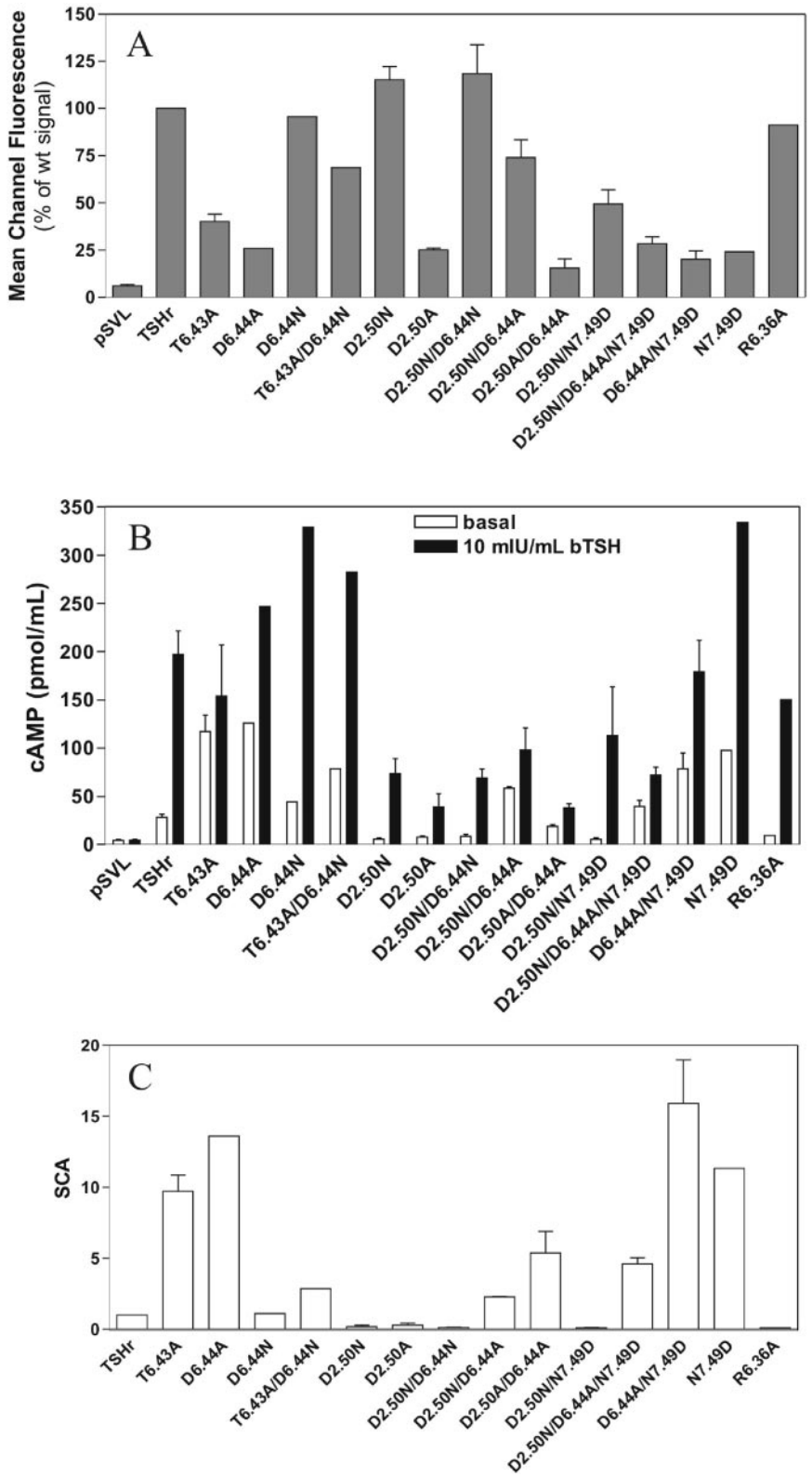

FIG. 2. **Asp-2.50, Asp-6.44, Arg-6.36, and Asn-7.49 mutants.** *A*, level of cell surface expression of the receptors in transfected COS cells determined by FACS. *B*, basal and bTSH induced intracellular cAMP accumulation measured in COS cells transfected with each receptor (bTSH was added at 10 mIU/ml during 1 h of incubation). *C*, constitutive activity normalized to surface expression according to the SCA calculation. These figures represent the data of experiments performed independently at least twice (results expressed as mean ± range of duplicates).

N7.49D double mutant receptor would involve conformational change of Asp-7.49 from pointing toward TM 6 down to the cytoplasmic side (Fig. 1, *c* and *d*). In this active conformation the $N_{\delta 2}H$ group of Asn-2.50 would act as a donor in the hydrogen bond interaction with the $O_{\delta 1}$ atom of Asp-7.49. Similarly to WT TSHr, the polar $O_{\delta 2}$ atom of Asp-7.49 would be accessible and pointing toward the intracellular side (Fig. 1, *b* and *d*).

*The Counterpart of Asp-2.50**Asn-7.49 in the Active State of the TSHr*—Our various simulations (Fig. 1) indicate that upon formation of the 2.50**7.49 interaction in WT TSHr or D2.50N and D2.50N/N7.49D mutants the O_{δ} atom of Asn-7.49 or Asp-7.49 points toward the intracellular side. Fig. 1, *e–g*, shows the resulting molecular electrostatic potential of the receptor structure at the accessible surfaces of Asn-7.49 or Asp-7.49 (see "Experimental Procedures"). Clearly, because of the presence of the negatively charged Asp-2.50, the O_{δ} atom of Asn-7.49 is more polar than a regular carbonyl of neutral Asn (compare Fig. 1, *e* with *f*) and resembles the polarity of the negatively

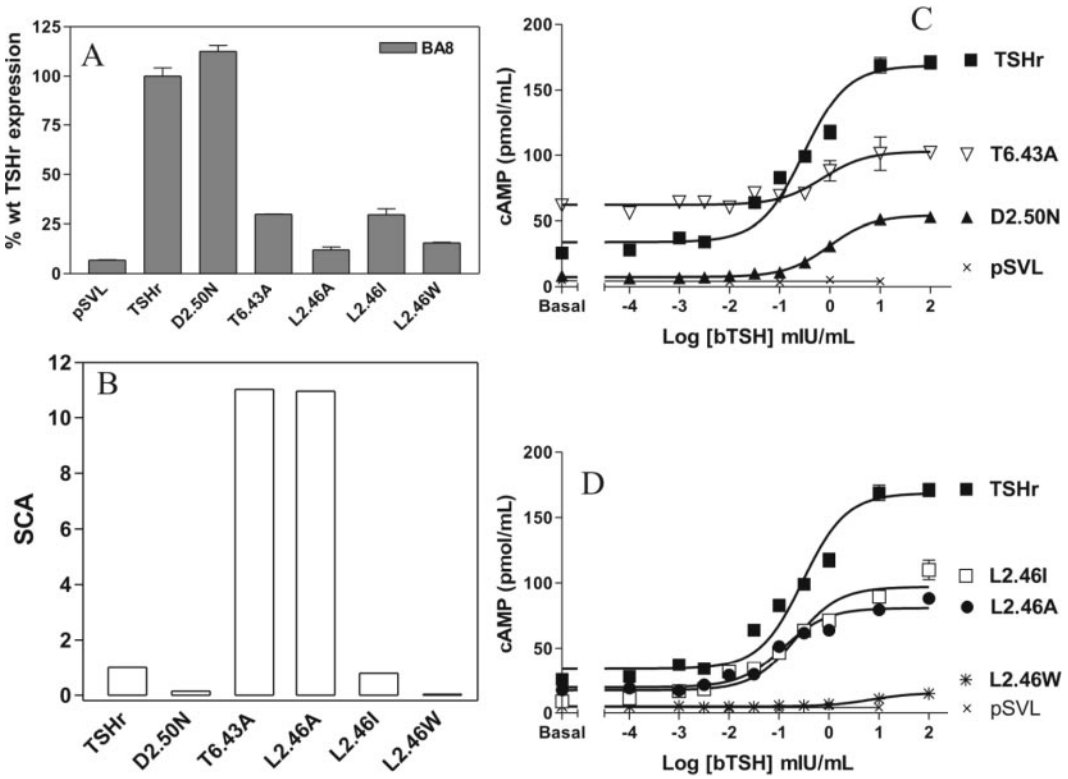

FIG. 3. **Concentration-response curves.** *A*, level of cell surface expression of the receptors in transfected COS cells determined by FACS. *B*, constitutive activity normalized to surface expression according to the SCA calculation. *C* and *D*, concentration-response curves for TSH and mutant receptors under stimulation by increasing concentrations of bTSH. Each curve is representative of at least two separate experiments. Results were analyzed by nonlinear regression using GraphPad Prism software.

charged O_δ atom of Asp-7.49 (Fig. 1, compare *f* with *g*). Furthermore, although D2.50A is still able to induce cAMP production in the presence of the ligand (Fig. 2), the N7.49A mutant cannot be activated by TSH (13). Thus, it seems reasonable to suggest that Asn-7.49 is a key residue in receptor activation, whereas the role of Asp-2.50 is to increase the reactivity of the O_δ atom of Asn-7.49 toward an intracellular counterpart (*i.e.* a positive charge, see below).

Although our MD simulations suggest that the nearby Arg-6.36 (specific to the glycoprotein hormone receptor family) could interact with the O_δ atom of Asn-7.49, the R6.36A mutant can still be activated by TSH ruling out this arginine as a key counterpart to the Asp-2.50**Asn-7.49 pair in the active state of the receptor. Still, we expect positively charged residue(s) to interacts with the acidic pocket described above.

It had been suggested that the highly conserved Arg-3.50 of the (D/E)RY motif at the bottom of TM 3 also performs a conformational change during the process of receptor activation: the ionic counterpart of Arg-3.50 in the inactive state would be the contiguous D/Glu-3.49, replaced by Asp-2.50 in the active state (38). This appears currently unlikely, as the D2.50A mutant is still activable. However, the charged side chain of Arg-3.50 could be the ionic counterpart of the Asp-2.50**Asn-7.49 pair, interacting with the closer and polar O_δ atom of Asn-7.49. This hypothesis is also supported by the fact that addition of the N7.49A mutation to the constitutively active E3.49A or E3.49Q mutant receptors, dramatically lowers their activity to levels of wild type TSHr (25). Thus, the release of the Arg-3.50 side chain by either E3.49A or E3.49Q mutations is only stable in the presence of Asn-7.49, which could indicate a direct Arg-3.50**Asn-7.49 interaction. Moreover, a conformational link between Asp-2.50, Arg-3.50, and Tyr-5.58 has been shown to be critical for muscarinic M_3 receptor activation (39). However, it is important to note that large conformational changes of TM 3, TM 6, and TM 7 are required to bring the side chains of Arg-3.50 and Asn-7.49 into proximity. Importantly, cross-linking studies of rhodopsin indicate that such a large conformational change of TM 3 toward TM 7 occurs upon activation (40).

Alternatively, the putative positive charge supposed to be the counterpart of Asn-7.49 in the active state could also be located in the G protein. This would be in agreement with previous data suggesting that Asn-7.49 in the cholecystokinin B receptor is specifically involved in G_q protein activation (41). In this receptor, the N7.49A mutant keeps similar expression levels and high affinity cholecystokinin binding compared with WT receptor. It can form stable complexes with G_q upon ligand binding but lacks the ability to activate phospholipase C and protein kinase C.

The Role of the Highly Conserved Leu-2.46 in the Process of TSHr Activation—Leu-2.46 is part of the (N/S)L*xxx*D motif in TM 2, highly conserved among all the members of the rhodopsin-like family of GPCR. Until now, only one group has reported mutagenesis data on Leu-2.46 mutants in rhodopsin (42). Similar to their findings, the L2.46A single mutant in the TSHr shows a significant increase in constitutive activity by a factor of ~13, relative to wild type TSHr (Table I and Fig. 3). The removal of the side chain (mutation into Ala) implies the loss of an interaction important for keeping the inactive state. Leu-2.46 belongs to a cluster of hydrophobic residues (43). It was suggested that to enable the movement of TM 3 and 6, necessary for receptor activation, hydrophobic contacts in this cluster might undergo a rearrangement (34). Madabushi *et al.* (42) extended this idea by suggesting that the signal originating from ligand binding would be transduced through this core toward the G protein-coupling site.

Considering the effect of the L2.46A mutation in constitutive activity of the TSHr, comparable in magnitude to the T6.43A,

D6.44A, or N7.49D mutants, it is tempting to propose an alternative role for Leu-2.46 in the activation mechanism. The allowed conformations of Leu in α-helices are restricted to *gauche*+ and *trans* rotamers (44). In the *gauche*+ rotamer (observed in rhodopsin), the side chain of Leu-2.46 points toward TM 3 and away from the Asn-7.49**Asp-2.50 pair. In *trans* conformation the side chain of Leu-2.46 would be located halfway between Asp-2.50 and Asn-7.49 and, thus, interfering with the conformational transition of Asn-7.49. Therefore, the bulky and γ-branched Leu-2.46 could also constrain the conformation of Asn-7.49 toward TM 6 by occupying the space between Asn-7.49 and Asp-2.50 in the TSHr. However, additional knowledge of the residues participating in the network of interactions that stabilize the active conformation of the receptor is indispensable for further understanding the active role of Leu-2.46.

Conclusions—The rhodopsin family of GPCRs is characterized by a number of highly conserved charged and polar residues located within the TM region. Mutagenesis studies indicate that most if not all of these amino acids are involved in the activation mechanism. Our work aimed at understanding the molecular roles and relationships of these residues and their conformational regulation during receptor activation. The highly conserved Asn-7.49 appears to have a well defined inactive conformation, locked by interactions that are specific to each subfamily. Upon activation, it must reorient toward another conserved residue, Asp-2.50. This combination of polar and charged side chains leads to a particular electrostatic landscape, which, in our view, is at the center of receptor activation. The highly negative potential produced in the TM 2–TM 3 region could force reorientation of another highly conserved charge, Arg-3.50, and drive the important conformational reorganization of the TM bundle. Alternatively, negative electrostatics could be directly involved in the interaction with the G protein. As these key residues are common to all rhodopsin-like GPCRs, we believe that these molecular steps form a conserved mechanism.

Acknowledgment—We thank Joost J. J. van Durme for helpful discussions.

REFERENCES

1. Fredriksson, R., Lagerstrom, M. C., Lundin, L. G., and Schioth, H. B. (2003) *Mol. Pharmacol.* **63,** 1256–1272
2. Bockaert, J., and Pin, J. P. (1999) *EMBO J.* **18,** 1723–1729
3. Kristiansen, K. (2004) *Pharmacol. Ther.* **103,** 21–80
4. Palczewski, K., Kumasaka, T., Hori, T., Behnke, C. A., Motoshima, H., Fox, B. A., Trong, I. L., Teller, D. C., Okada, T., Stenkamp, R. E., Yamamoto, M., and Miyano, M. (2000) *Science* **289,** 739–745
5. Li, J., Edwards, P. C., Burghammer, M., Villa, C., and Schertler, G. F. (2004) *J. Mol. Biol.* **343,** 1409–1438
6. Mirzadegan, T., Benko, G., Filipek, S., and Palczewski, K. (2003) *Biochemistry* (*Mosc.*) **42,** 2759–2767
7. Samama, P., Cotecchia, S., Costa, T., and Lefkowitz, R. J. (1993) *J. Biol. Chem.* **268,** 4625–4636
8. Liapakis, G., Chan, W. C., Papadokostaki, M., and Javitch, J. A. (2004) *Mol. Pharmacol.* **65,** 1181–1190
9. Kobilka, B. (2004) *Mol. Pharmacol.* **65,** 1060–1062
10. Swaminath, G., Xiang, Y., Lee, T. W., Steenhuis, J., Parnot, C., and Kobilka, B. K. (2004) *J. Biol. Chem.* **279,** 686–691
11. Shi, L., Liapakis, G., Xu, R., Guarnieri, F., Ballesteros, J. A., and Javitch, J. A. (2002) *J. Biol. Chem.* **277,** 40989–40996
12. Ruprecht, J. J., Mielke, T., Vogel, R., Villa, C., and Schertler, G. F. (2004) *EMBO J.* **23,** 3609–3620
13. Govaerts, C., Lefort, A., Costagliola, S., Wodak, S., Ballesteros, J. A., Pardo, L., and Vassart, G. (2001) *J. Biol. Chem.* **276,** 22991–22999
14. Okada, T., Fujiyoshi, Y., Silow, M., Navarro, J., Landau, E. M., and Shichida, Y. (2002) *Proc. Natl. Acad. Sci. U. S. A.* **99,** 5982–5987
15. Ballesteros, J. A., Jensen, A. D., Liapakis, G., Rasmussen, S. G., Shi, L., Gether, U., and Javitch, J. A. (2001) *J. Biol. Chem.* **276,** 29171–29177
16. Prioleau, C., Visiers, I., Ebersole, B. J., Weinstein, H., and Sealfon, S. C. (2002) *J. Biol. Chem.* **277,** 36577–36584
17. Fritze, O., Filipek, S., Kuksa, V., Palczewski, K., Hofmann, K. P., and Ernst, O. P. (2003) *Proc. Natl. Acad. Sci. U. S. A.* **100,** 2290–2295
18. Farrens, D. L., Altenbach, C., Yang, K., Hubbell, W. L., and Khorana, H. G. (1996) *Science* **274,** 768–770
19. Meng, E. C., and Bourne, H. R. (2001) *Trends Pharmacol. Sci.* **22,** 587–593
20. Smits, G., Campillo, M., Govaerts, C., Janssens, V., Richter, C., Vassart, G., Pardo, L., and Costagliola, S. (2003) *EMBO J.* **22,** 2692–2703
21. Vassart, G., Pardo, L., and Costagliola, S. (2004) *Trends Biochem. Sci.* **29,** 119–126
22. Parma, J., Duprez, L., Van Sande, J., Hermans, J., Rocmans, P., Van Vliet, G., Costagliola, S., Rodien, P., Dumont, J. E., and Vassart, G. (1997) *J. Clin. Endocrinol. Metab.* **82,** 2695–2701
23. Angelova, K., Narayan, P., Simon, J. P., and Puett, D. (2000) *Mol. Endocrinol.* **14,** 459–471
24. Angelova, K., Fanelli, F., and Puett, D. (2002) *J. Biol. Chem.* **277,** 32202–32213
25. Claeysen, S., Govaerts, C., Lefort, A., Van Sande, J., Costagliola, S., Pardo, L., and Vassart, G. (2002) *FEBS Lett.* **517,** 195–200
26. Whistler, J. L., Gerber, B. O., Meng, E. C., Baranski, T. J., von Zastrow, M., and Bourne, H. R. (2002) *Traffic* **3,** 866–877
27. Ballesteros, J. A., and Weinstein, H. (1995) *Methods Neurosci.* **25,** 366–428
28. Case, D. A., Darden, T. A., Cheatham, T. E., III, Simmerling, C. L., Wang, J., Duke, R. E., Luo, R., Merz, K. M., Wang, B., Pearlman, D. A., Crowley, M., Brozell, S., Tsui, V., Gohlke, H., Mongan, J., Hornka, V., Cui, G., Beroza, P., Schafmeister, C., Caldwell, J. W., Ross, W. S., and Kollman, P. A. (2003), AMBER 8, University of California, San Francisco
29. Wang, J., Cieplak, P., and Kollman, P. A. (2000) *J. Comput. Chem.* **21,** 1049–1074
30. Nicholls, A., Sharp, K. A., and Honig, B. (1991) *Proteins* **11,** 281–296
31. Costagliola, S., Rodien, P., Many, M. C., Ludgate, M., and Vassart, G. (1998) *J. Immunol.* **160,** 1458–1465
32. Vlaeminck-Guillem, V., Ho, S. C., Rodien, P., Vassart, G., and Costagliola, S. (2002) *Mol. Endocrinol.* **16,** 736–746
33. Montanelli, L., Van Durme, J. J., Smits, G., Bonomi, M., Rodien, P., Devor, E. J., Moffat-Wilson, K., Pardo, L., Vassart, G., and Costagliola, S. (2004) *Mol. Endocrinol.* **18,** 2061–2073
34. Okada, T., and Palczewski, K. (2001) *Curr. Opin. Struct. Biol.* **11,** 420–426
35. Neumann, S., Krause, G., Chey, S., and Paschke, R. (2001) *Mol. Endocrinol.* **15,** 1294–1305
36. Zhou, W., Flanagan, C., Ballesteros, J. A., Konvicka, K., Davidson, J. S., Weinstein, H., Millar, R. P., and Sealfon, S. C. (1994) *Mol. Pharmacol.* **45,** 165–170
37. Sealfon, S. C., Chi, L., Ebersole, B. J., Rodic, V., Zhang, D., Ballesteros, J. A., and Weinstein, H. (1995) *J. Biol. Chem.* **270,** 16683–16688
38. Ballesteros, J., Kitanovic, S., Guarnieri, F., Davies, P., Fromme, B. J., Konvicka, K., Chi, L., Millar, R. P., Davidson, J. S., Weinstein, H., and Sealfon, S. C. (1998) *J. Biol. Chem.* **273,** 10445–10453
39. Li, B., Nowak, N. M., Kim, S. K., Jacobson, K. A., Bagheri, A., Schmidt, C., and Wess, J. (2005) *J. Biol. Chem.* **280,** 5664–5675
40. Yu, H., Kono, M., and Oprian, D. D. (1999) *Biochemistry* (*Mosc.*) **38,** 12028–12032
41. Gales, C., Kowalski-Chauvel, A., Dufour, M. N., Seva, C., Moroder, L., Pradayrol, L., Vaysse, N., Fourmy, D., and Silvente-Poirot, S. (2000) *J. Biol. Chem.* **275,** 17321–17327
42. Madabushi, S., Gross, A. K., Philippi, A., Meng, E. C., Wensel, T. G., and Lichtarge, O. (2004) *J. Biol. Chem.* **279,** 8126–8132
43. Horn, F., Bettler, E., Oliveira, L., Campagne, F., Cohen, F. E., and Vriend, G. (2003) *Nucleic Acids Res.* **31,** 294–297
44. Dunbrack, R. L. J., and Cohen, F. E. (1997) *Protein Sci.* **6,** 1661–1681
45. Kraulis, J. (1991) *J. Appl. Crystallogr.* **24,** 946–950
46. Merritt, E. A., and Bacon, D. J. (1997) *Methods Enzymol.* **277,** 505–524